



# High-resolution, three-dimensional modeling of human leukocyte antigen class I structure and surface electrostatic potential reveals the molecular basis for alloantibody binding epitopes

Vasilis Kosmoliaptis<sup>a,b,\*</sup>, Timothy R. Dafforn<sup>c</sup>, Afzal N. Chaudhry<sup>d</sup>, David J. Halsall<sup>e</sup>, J. Andrew Bradley<sup>b</sup>, Craig J. Taylor<sup>a</sup>

<sup>a</sup> Tissue Typing Laboratory, Cambridge University Hospitals NHS Foundation Trust, Addenbrooke's Hospital, Cambridge, England

<sup>b</sup> Department of Surgery, University of Cambridge, Addenbrooke's Hospital, Cambridge, England

<sup>c</sup> School of Biosciences, University of Birmingham, Edgbaston, Birmingham, England

<sup>d</sup> Department of Renal Medicine, Cambridge University Hospitals NHS Foundation Trust, Addenbrooke's Hospital, Cambridge, England

<sup>e</sup> Department of Clinical Biochemistry, Cambridge University Hospitals NHS Foundation Trust, Addenbrooke's Hospital, Cambridge, England

## ARTICLE INFO

### Article history:

Received 21 December 2010

Accepted 5 July 2011

Available online 28 July 2011

### Keywords:

Alloantigen immunogenicity

HLA antibodies

## ABSTRACT

The potential of human leukocyte antigens (HLA) to stimulate humoral alloimmunity depends on the orientation, accessibility and physiochemical properties of polymorphic amino acids. We have generated high-resolution structural and physiochemical models of all common HLA class I alleles and analyzed the impact of amino acid polymorphisms on surface electrostatic potential. Atomic resolution three-dimensional structural models of HLA class I molecules were generated using the MODELLER computer algorithm. The molecular surface electrostatic potential was calculated using the DelPhi program. To confirm that electrostatic surface topography reflects known HLA B cell epitopes, we examined Bw4 and Bw6 and ascertained the impact of amino acid polymorphisms on their tertiary and physiochemical composition. The HLA protein structures generated performed well when subjected to stereochemical and energy-based testing for structural integrity. The electrostatic pattern and conformation of Bw4 and Bw6 epitopes are maintained among HLA molecules even when expressed in a different structural context. Importantly, variation in epitope amino acid composition does not always translate into a different electrostatic motif, providing an explanation for serologic cross-reactivity. Mutations of critical amino acids that abrogate antibody binding also induce distinct changes in epitope electrostatic properties. In conclusion, high-resolution structural modeling provides a physiochemical explanation for serologic patterns of antibody binding and provides novel insights into HLA immunogenicity.

© 2011 Published by Elsevier Inc. on behalf of American Society for Histocompatibility and Immunogenetics.

## 1. Introduction

Elucidation of the crystallographic structure of human leukocyte antigen (HLA) class I and II more than 20 years ago contributed immeasurably to understanding of the relationship between structure and function of HLA [1,2]. Since then, advances in molecular sequencing technology have enabled resolution at the amino acid sequence level of more than 2000 different HLA alleles and this has led to better understanding of the role of HLA in health and disease, and in the field of tissue transplantation has allowed improved definition of HLA incompatibilities between transplant donors and recipients.

Knowledge of the amino acid sequence of an HLA allele allows insight into its potential peptide binding repertoire and in the context of transplantation, comparison of the sequences of differ-

ent HLA alleles enables prediction of immunogenicity of a particular HLA mismatch [3–5]. Amino acid sequence alone, although it is useful, provides limited insight into the molecular basis of protein–protein interactions that are mediated in large part by electrostatic properties; [6–8] electrostatic forces are particularly important determinants of the specificity and affinity of alloantibody binding [9,10]. The electrostatic properties of HLA are determined by the number and distribution of polar and charged amino acid residues, and integration of this information in structural models of HLA combined with application of electrostatic theory to biologic macromolecules enable the three-dimensional (3D) topographic distribution of electrostatic potential to be determined [11,12].

We describe here the use of comparative protein structure modeling, based on available crystallographic data and amino acid sequence data, to generate high-resolution structural and physicochemical models of all the common HLA class I alleles. The structural HLA class I models generated allowed the impact of

\* Corresponding author.

E-mail address: [kosmo@doctors.org.uk](mailto:kosmo@doctors.org.uk) (V. Kosmoliaptis).

single and multiple amino acid polymorphisms on surface electrostatic potential to be visualized and this provided an explanation at the molecular level for alloantibody binding patterns to known HLA epitopes, as well as to epitopes not previously explicable by amino acid sequence alone.

## 2. Subjects and methods

### 2.1. Strategy for generating structural and physiochemical models of HLA class I alleles

A limited number of HLA class I molecular structures have been resolved to a high resolution by X-ray crystallography and this information was used together with amino acid sequence data to generate, by comparative protein structure modeling (homology modeling), atomic resolution structural models of all the common HLA-A, -B, and -C alleles. Because we were interested primarily in understanding the effects of HLA polymorphism on the ability of HLA molecules to interact with other proteins (e.g., alloantibodies) in which electrostatic forces play a major role, the electrostatic potential at the molecular surface of the different HLA alleles was calculated and depicted in 3D images.

### 2.2. 3D protein structure modeling of HLA class I alloantigens

HLA class I molecular structures, resolved by X-ray crystallography, were obtained from the Protein Data Bank (PDB; <http://www.rcsb.org/pdb/>), and homology modeling was used to determine the atomic coordinates of the most common HLA-A, -B, and -C molecules by satisfaction of spatial restraints as implemented in the MODELLER computer algorithm [13]. Where described, the structural impact of amino acid residue mutations introduced in certain HLA proteins was determined using the same protocol. Both a manual and a PSI-BLAST [14] search (using the HLA-A\*01:01 as the query sequence) against the PDB was performed to identify suitable HLA proteins of known structure for use as global templates for modeling. The initial query identified 115 candidate template structures, which were evaluated for structural quality based on their atomic resolution, R-factor, and total number of crystallographically resolved residues (completeness of data). In cases of independent determinations of the same HLA allele, the structure with the higher quality indicators was selected. Template structures were further assessed for stereochemical quality using the WHAT\_CHECK and PROCHECK verification algorithms and by inspection of the Ramachandran plots [15–18]. Accordingly, 11 HLA class I structures with the highest stereochemical scores and finest atomic resolution ( $\leq 2 \text{ \AA}$ ) were selected as templates to increase the accuracy of the comparative modeling procedure (PDB entries: 1XH3, 2CIK, 1ZHL, 2NW3, 1M6O, 1SYV, 2HJL, 2BVP, 1K5N, 1X7Q, and 1I4F).

The amino acid sequences of all serologically defined HLA class I molecules were obtained from the IMGT/HLA database (<http://www.ebi.ac.uk/imgt/hla/>). Multiple sequence alignments were performed using the CLUSTALX v. 1.83 [19] software and manually corrected where indicated. The alignment files were then entered into the MODELLER program to construct 3D HLA class I models. In brief, MODELLER generates the 3D atomic coordinates of the target sequences by satisfying spatial restraints, obtained from the templates, and by Chemistry at Harvard Macromolecular Mechanics (CHARMM) energy terms enforcing proper stereochemistry; [20] an optimization is then carried out by using methods of conjugate gradients and molecular dynamics with simulated annealing [21].

### 2.3. Electrostatic potential calculations

The electrostatic potential around the 3D structures (obtained from homology modeling) of HLA class I molecules was computed by numerically solving the Poisson Boltzmann equation using the finite difference method implemented in the DelPhi program

[22,23] within Discovery Studio 2.1 (Accelrys Inc, San Diego, CA), as described in the Supplementary methods section.

To enable accurate structure prediction and electrostatic potential calculation, an alanine nonamer peptide was fitted in the peptide binding groove of all modeled HLA structures based on the crystallographic atomic coordinates of the peptides presented in the groove of the template structures.

## 3. Results

The focus of this study was to generate atomic resolution 3D structural models of all common HLA class I molecules and calculate the electrostatic potential at their molecular surface. To confirm that the HLA electrostatic surface topography reflects known B cell epitopes, we examined well characterized B cell epitopes and ascertained the impact of amino acid polymorphisms on their tertiary and physiochemical composition. We studied the serologically defined HLA Bw4 and Bw6 B cell epitopes expressed on different HLA molecules to provide a molecular explanation for previously described patterns of antibody reactivity.

### 3.1. Validation of structural quality of modeled HLA molecules

The stereochemical quality of the modeled structures was assessed using the WHAT\_CHECK [15] and PROCHECK [16] algorithms. Both algorithms calculate a variety of stereochemical and geometrical parameters based on a structure's atomic coordinates and assess them according to theoretic calculations and by comparison to standard values obtained from regularly updated databases of high quality, experimentally resolved structures. Commonly assessed parameters include the Ramachandran plot quality (examines whether main chain residues adopt torsion angles compatible with the secondary structure they are part of, without leading to steric clashes), normality of bond angles and bond lengths, side chain torsion angle distribution (chi and omega angles) and chirality and planarity checks. The PROCHECK and WHAT\_CHECK outputs for representative HLA structures are shown in Supplementary Tables 1 and 2. Overall, homology models achieved high scores for the parameters assessed by both algorithms. None of the modeled structures had residues in sterically disallowed areas of the Ramachandran plots (Supplementary Fig. 1). All modeled HLA structures were also examined for protein folding quality using empiric energy potentials as implemented in the ProSA algorithm [24,25]. The program evaluates the energy of a structure using distance-based pair potentials and a potential that captures the solvent exposure of the protein's residues. Misfolded regions are recognized by abnormally high energy values. Inspection of ProSA residue energy plots did not reveal any misfolded regions, and the total ProSA energy value for each structure was within the expected range derived from similar size experimentally determined protein structures deposited in the PDB (Supplementary Fig. 2).

### 3.2. Electrostatic analysis and structural characteristics of Bw6 epitope

Bw6 is a well-characterized serologic public B cell epitope determined by a sequence motif between residues 77 and 83 expressed on the carboxyl terminal of the  $\alpha 1$  helix of HLA-B alleles [26,27]. To study the conformational and physiochemical characteristics of the Bw6 epitope, the structures of common Bw6-expressing HLA-B molecules were modeled and their molecular electrostatic potential determined. The position and structural architecture of Bw6 as expressed on HLA-B\*07:02 molecule is shown in Fig. 1a and depicted in expanded form in Fig. 1b. The solvent accessible area of the Bw6 epitope is defined predominantly by Arg79, Asn80, Arg82, and Gly83 (Fig. 1a, Supplementary Table 3). Although the Glu76 residue is outside the canonical Bw6 motif, it constitutes a critical part of the epitope because of the position of its amino acid side chain in relation to residues 77–80 and its

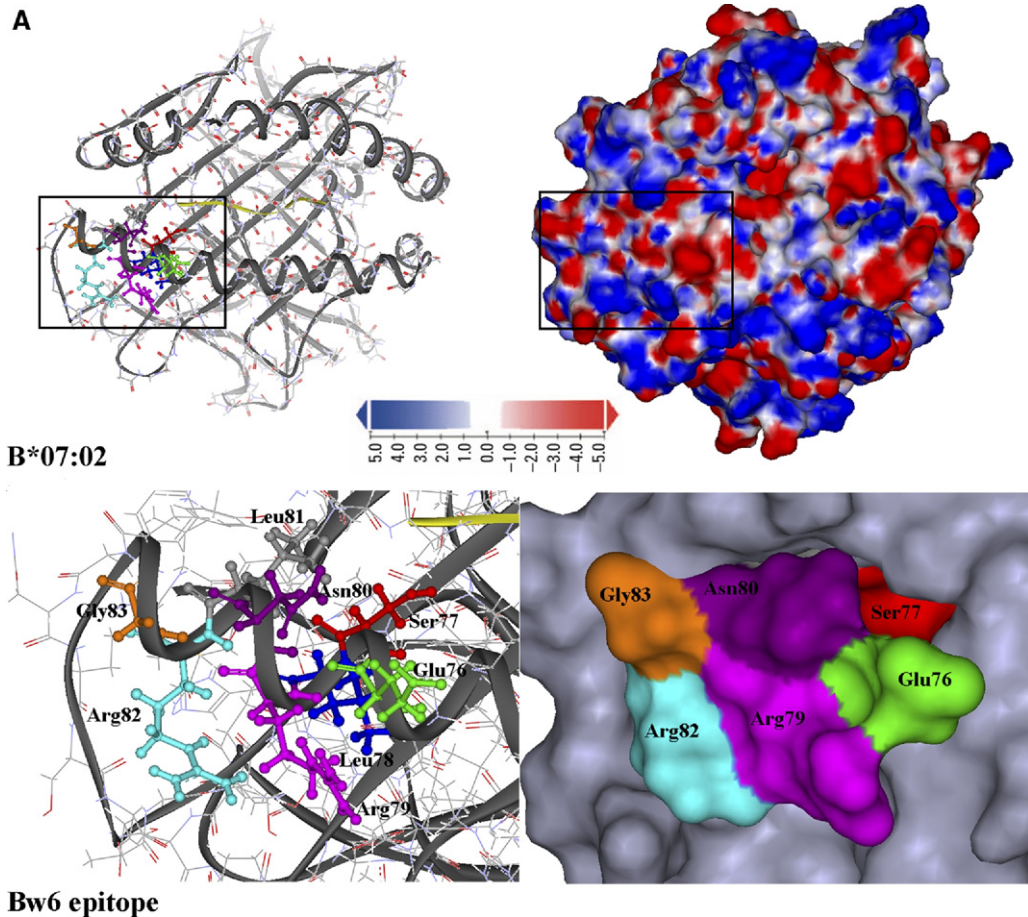


**Fig. 1.** Tertiary structure and molecular surface electrostatic potential of Bw6 epitope. (a) Residues 77–83 constitute the Bw6 epitope. The area included in the frame (Bw6) is shown (in expanded form) in panel b for all modeled Bw6 expressing HLA molecules. The structure of the epitope is depicted in ball-and-stick representation and also the solvent accessible surface of the epitope is colored to reveal the relevant contribution of each residue. (b) “Birds-eye-view” of the Bw6 epitope on different HLA molecules (rectangle area in panel a expanded). All structures were superimposed on HLA-B\*07:02 and therefore depict the same view. The solvent accessible surface of the epitope is colored according to the calculated electrostatic potential. Electrostatic potentials less than  $-5 \text{ kT/e}$  are colored red, those greater than  $5 \text{ kT/e}$  blue, and neutral potentials ( $0 \text{ kT/e}$ ) are colored white. Linear interpolation was used to produce the color for surface potentials between these values (see color scale, panel a).

surface accessibility (further analyzed below). The side chain of serine77 is oriented toward the peptide-binding groove and has limited surface accessibility in all HLA-B molecules examined (Supplementary Table 3). Similarly, the side chains of Leu78 and Leu81 are oriented toward the  $\beta$ -pleated sheet and peptide binding groove, respectively.

The surface electrostatic potential of the Bw6 epitope expressed on a representative selection of common HLA-B alleles is shown in Fig. 1b. Overall, the total solvent accessible area of the Bw6 epitope was very similar on all Bw6 expressing HLA-B molecules and ranged from 327 to 384  $\text{\AA}^2$  (mean: 351  $\text{\AA}^2$ , standard deviation [SD], 19). It is apparent that the Bw6 epitope has remarkably consistent structural expression and electrostatic properties across all HLA-B molecules shown in Fig. 1b (this was the case for all common Bw6-expressing HLA-B molecules; data not shown). This topographic 3D pattern constitutes an electrostatic motif that is maintained despite the variability of amino acid polymorphisms surrounding the epitope and the disparate structural context of its expression on different HLA proteins, suggesting a uniform biologic behavior and explaining well-known homogeneous patterns of serologic reactivity. Even though the architecture of the Bw6 electrostatic motif is conserved, small differences among the HLA molecules examined do exist; whether this variation is of functional importance is uncertain and merits further study.

Serologic studies have shown that HLA-B\*46:01, -B\*73:01, and -B\*18:06 do not exhibit reactivity with Bw6 specific alloantibodies

and monoclonal antibodies even though they possess the canonical Bw6 motif at sequence positions 77–83 [28–30]. Based on sequence information, this has been attributed to an amino acid replacement at position 76 (glutamic acid to valine); however, the structural implications of this substitution have not been studied previously. To analyze the role of position 76 on the conformation and physiochemical characteristics of the Bw6 epitope, the structure and electrostatic potential of HLA-B\*18:06, -B\*46:01, and -B\*73:01 were analyzed and compared with that of HLA-B\*18:01. As shown in Figs. 2a and 2b, Val76 markedly alters the conformation and electrostatic motif of the Bw6 epitope expressed on HLA-B\*18:06, -B\*46:01, and -B\*73:01, thereby accounting for the observed abrogation of Bw6 specific antibody binding. The mean electrostatic potential of the most solvent-accessible amino acid side chains that constitute the Bw6 epitope is shown in Table 1 for HLA-B\*18:01 and -B\*18:06 (which differ only at residue 76) and quantitatively reflect the impact of the Glu76 to Val76 substitution ( $-75 \text{ kT/e}$  and  $-12 \text{ kT/e}$ , respectively).

### 3.3. Electrostatic analysis and structural characteristics of Bw4 epitope

The Bw4 epitope is characterized by amino acid residues at positions 77–83 of the distal  $\alpha 1$  helix [26,27]. The majority of HLA alleles that express the Bw4 epitope incorporate the motifs T-A-L-R, I-A-L-R, and T-L-L-R at positions 80–83, and asparagine, serine,

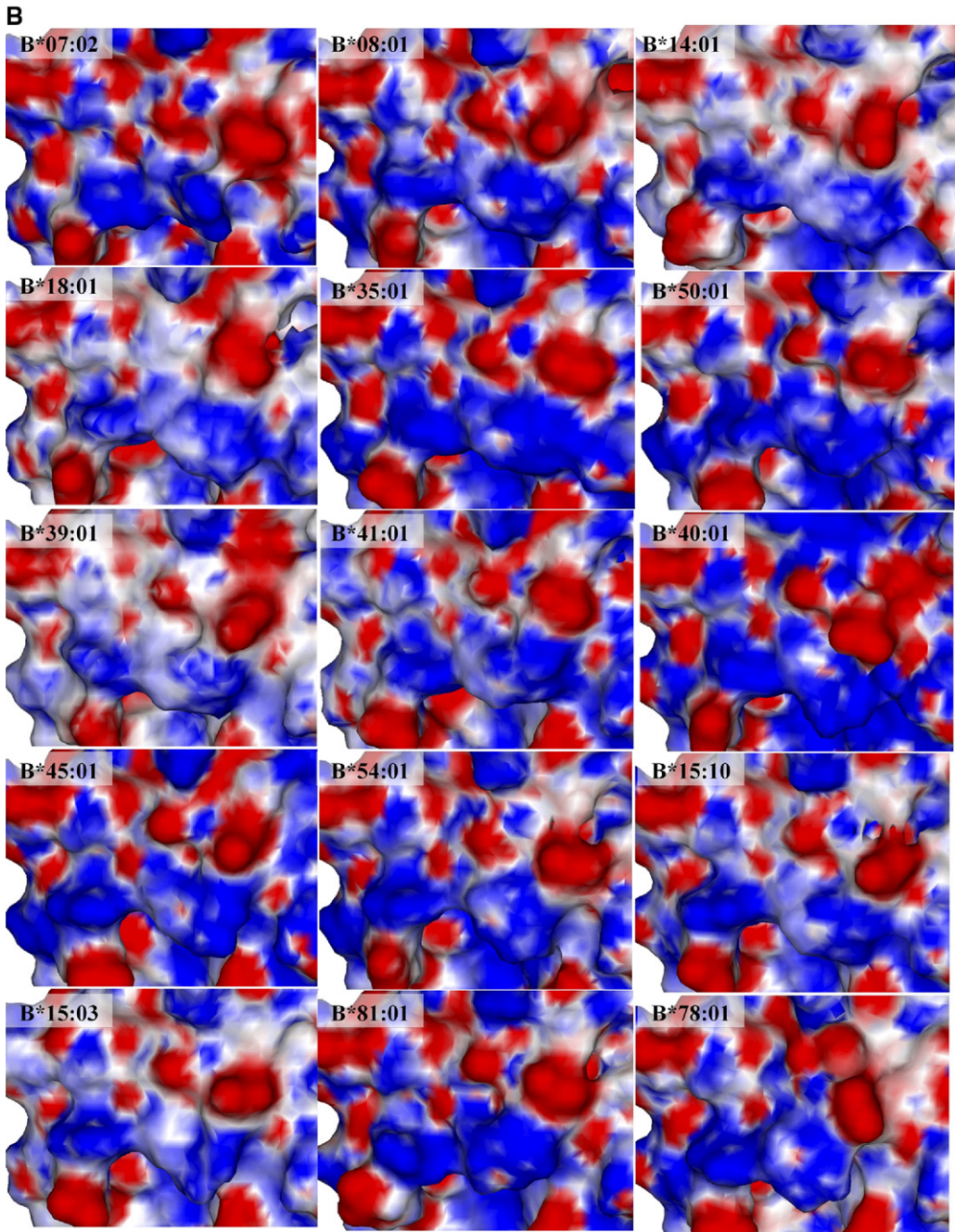


**Fig. 1.** (continued)

or aspartic acid at position 77 [30]. Differences in Bw4 specific alloantibody binding patterns are well documented among HLA specificities that express the Bw4 epitope [31,32]. The structural and physiochemical characteristics of the Bw4 epitope expressed on the common HLA-B alleles was modeled to determine whether the observed heterogeneity in Bw4 specific antibody binding patterns can be explained by differences in topography and surface electrostatic potential.

The position and structural architecture of the Bw4 epitope as expressed on HLA-B\*44:02 molecule is shown in Fig. 3a (and in expanded form in Fig. 3b). Analysis of solvent-accessibility showed that residues Arg79, Leu82, and Arg83 contribute most of the surface exposed area of the epitope, followed by threonine/isoleucine at position 80 (Fig. 3a, Supplementary Table 4). The polymorphic residue at position 77 is oriented toward the

peptide binding groove and has limited surface exposure (covered by the side chains of the alanine nonamer peptide) as is the case for Leu78 and Ala81/Leu81 that project toward the  $\beta$ -pleated sheet and are mainly covered by adjacent amino acid side chains.

Comparison of the surface electrostatic potential of the Bw4 epitope expressed on a representative selection of common HLA-B alleles showed that electrostatic patterns were broadly similar (Fig. 3b), although molecules expressing the I-A-L-R motif possessed unique electrostatic properties that distinguish them from molecules carrying the T-A-L-R and T-L-L-R motifs, and this is reflected in the alloantibody defined heterogeneity of Bw4. The I-A-L-R Bw4 motif is also expressed on a small number of HLA-A molecules (HLA-A23, A24, A25 and A32); modeling of these proteins showed that their Bw4 epitope has broadly similar electrostatic pattern to

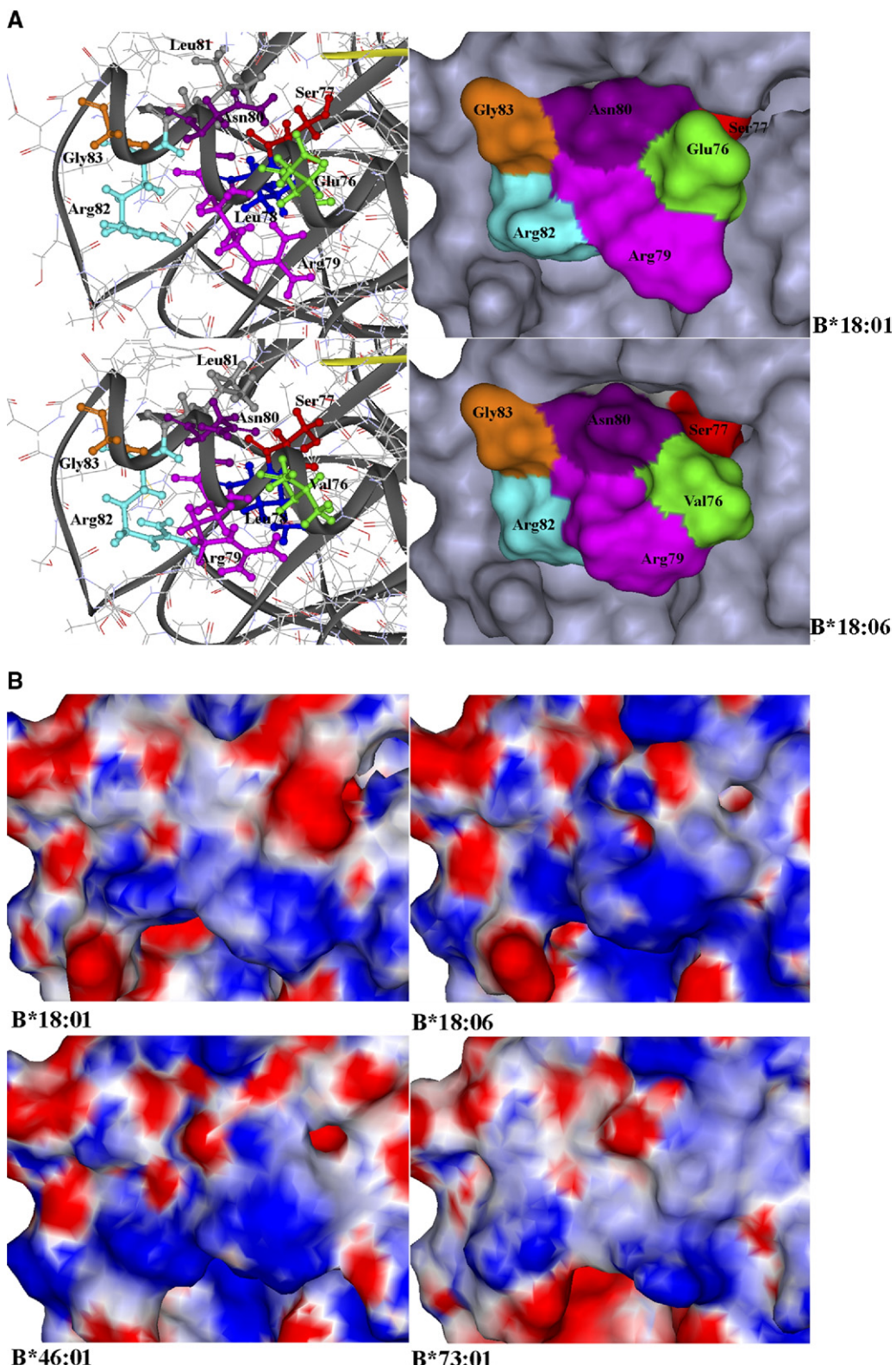


**Fig. 2.** Significance of residue 76 on Bw6 epitope. (a) The structure of Bw6 epitope on HLA-B\*18:01 and -B\*18:06 (ball-and-stick-representation and solvent accessible surface; the same rectangle area as in Fig. 1a is shown). (b) Bw6 epitope electrostatic potential for HLA-B\*18:01, -B\*18:06, -B\*46:01 and -B\*73:01. Glu76 to Val76 substitution markedly alters the electrostatic motif of the Bw6 epitope.

**Table 1**

Mean electrostatic potential of Bw6 epitope solvent accessible residues

Residue mean electrostatic potential (MEP in kT/e)					
Position	76	79	80	82	83
B*18: 01	E	R	N	R	G
MEP	−75.09	65.86	1.51	42.65	−10.05
B*18: 06	V	R	N	R	G
MEP	−11.71	79.53	26.38	52.94	−2.53

Mean electrostatic potential of the most solvent-accessible residues that constitute the Bw6 epitope is shown for HLA-B\*18:01 and -B\*18:06 whose amino acid sequences only differ at position 76.

the Bw4 epitope of HLA-B molecules expressing the I-A-L-R motif (data not shown).

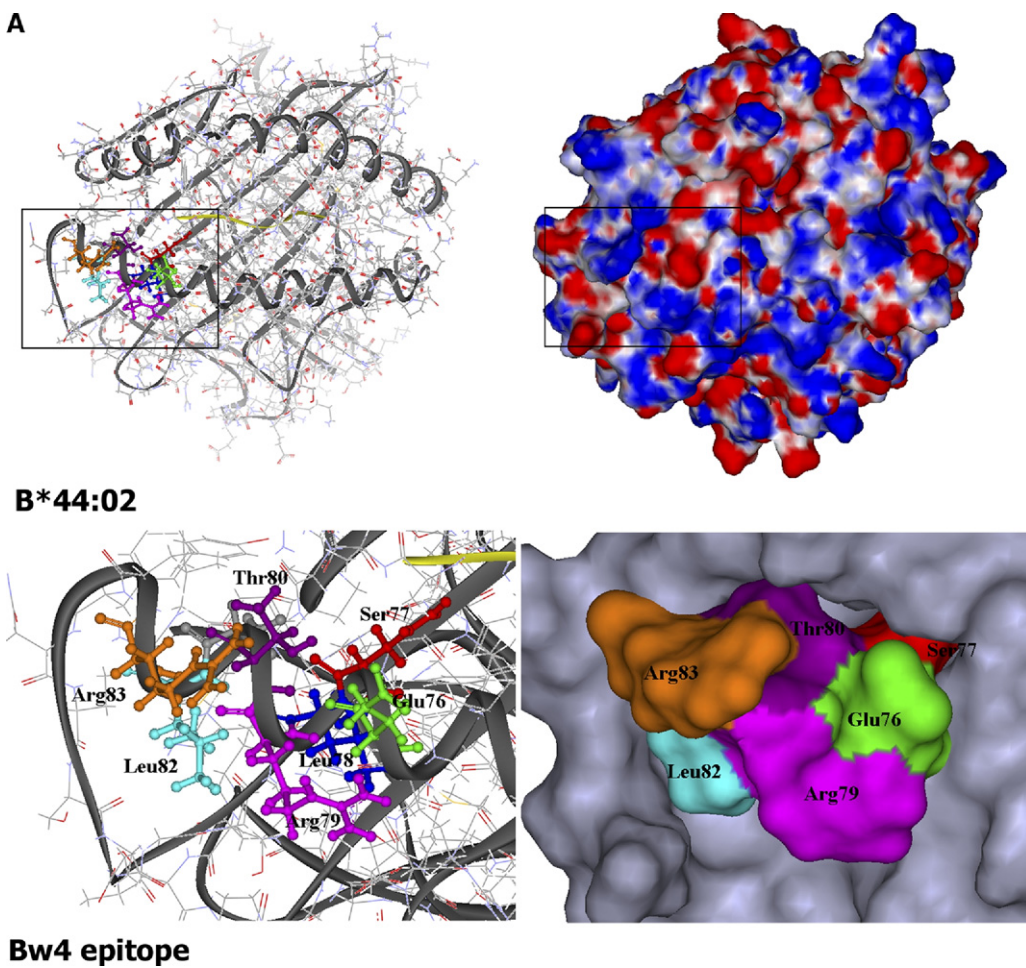
HLA-B\*44:02 and HLA-B\*13:01 alleles (T-A-L-R motif) and HLA-B\*27:05 and HLA-B\*47:01 (T-L-L-R motif) differ at position 77 of the Bw4 motif, expressing asparagine and aspartic acid, respectively, and showed almost identical Bw4 epitope electrostatic patterns. The minimal impact of residue 77 in this context is consistent with point mutagenesis studies that suggested position 77 is not critical for Bw4 monoclonal antibody binding [31]. Similarly, the alanine-to-leucine substitution at position 81 of the T-A-L-R and T-L-L-R motifs is conservative, has very limited side chain surface

accessibility and minimal effect on epitope structure and electrostatic potential.

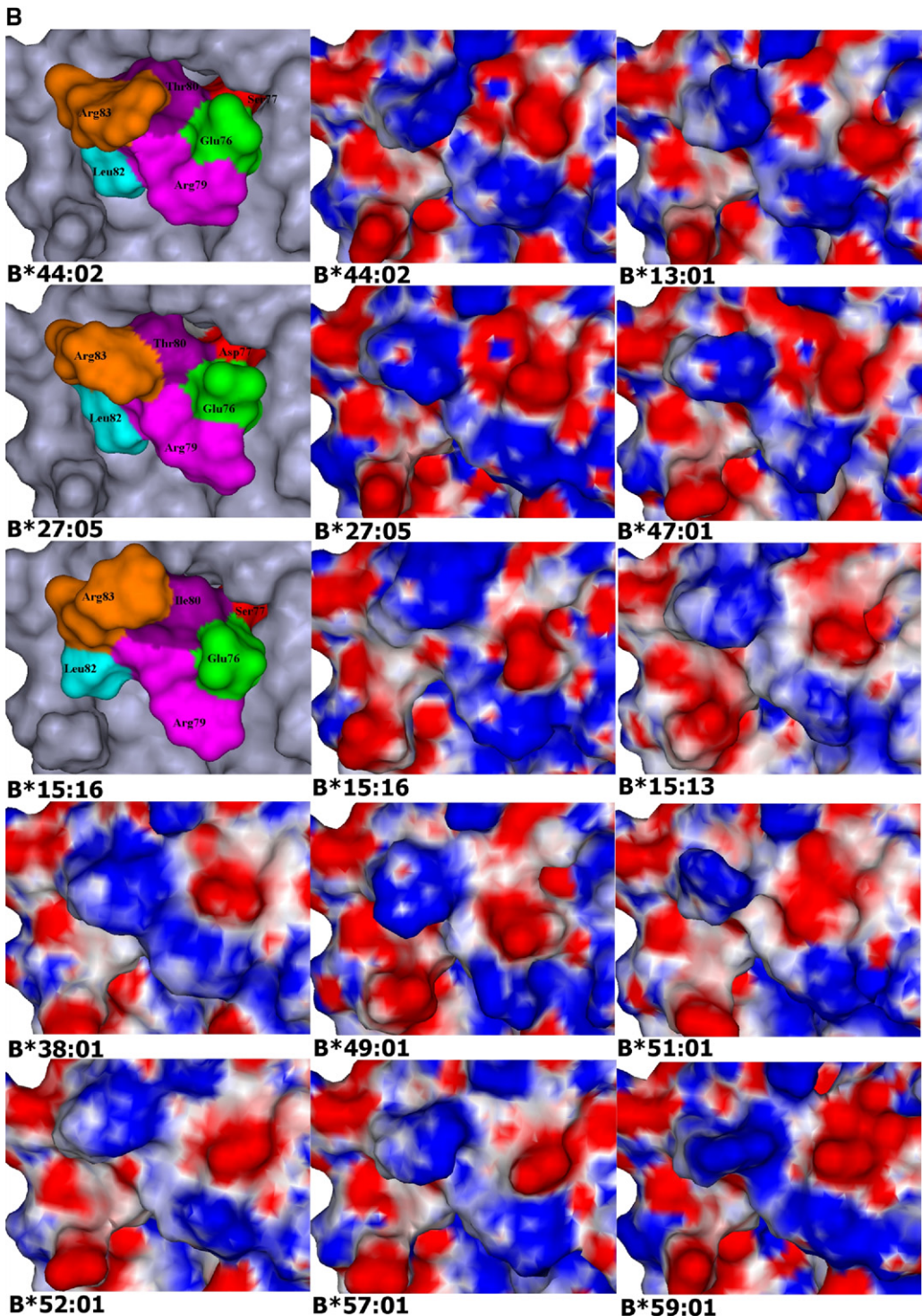
It has been shown previously that Bw4 specific alloantibodies show heterogeneous binding to Bw4 epitopes that have the same amino acid sequence motif but are expressed on different HLA-B alleles. For example, HLA-B\*44:02, B\*56:07, B\*08:02, and B\*18:09 have identical amino acid sequences at positions 77–83 that encompasses the Bw4 epitope, but that Bw4-specific antibodies bind strongly to B\*44:02 and B\*56:07 but only weakly to B\*08:02 and B\*18:09 (Fig. 4) [30,33]. The electrostatic models of the Bw4 epitope carried on the above four HLA alleles provide a likely explanation, revealing that amino acid polymorphisms outside the Bw4 motif, alter the electrostatic pattern and structural context of the Bw4 epitope (Fig. 4). HLA-B\*44:02 and B\*56:07 show almost identical electrostatic potential of the Bw4 epitope, whereas amino acid polymorphisms outside the Bw4 motif result in a distinct change to the electrostatic pattern of the Bw4 epitope on HLA-B\*08:02 and -B\*18:09.

#### 3.4. Structural and electrostatic analysis of point residue mutations that alter antibody reactivity with Bw6 epitope

We next applied the results from comparative models of HLA class I to provide a structural explanation of antibody binding



**Fig. 3.** Tertiary structure and molecular surface electrostatic potential of Bw4 epitope. (a) Residues 77–83 constitute the Bw4 epitope. Area included in frame (Bw4) is shown (in expanded form) in panel b for all modeled Bw4 expressing HLA molecules. The structure of the epitope is depicted in ball-and-stick representation and also the solvent accessible surface of the epitope is colored to reveal the relevant contribution of each residue. (b) The images show the “birds-eye-view” of the Bw4 epitope on different HLA molecules (rectangle area in panel a expanded). All structures were superimposed on HLA-B\*44:02 and therefore depict the same view. The solvent accessible surface of the epitope is colored according to the calculated electrostatic potential (as in Fig. 1). HLA-B molecules with the T-A-L-R and T-L-L-R Bw4 motifs (HLA-B\*44:02, -B\*13:01, -B\*27:05 and -B\*47:01) possess a similar electrostatic pattern, despite the polymorphisms at positions 77 and 81. HLA-B molecules expressing the I-A-L-R motif have uniform electrostatic properties that are distinguishable from those of T-A-L-R and T-L-L-R expressing HLA molecules suggesting Bw4 epitope heterogeneity.

**Fig. 3.** (continued)

patterns to previously reported mutant HLA alleles. Amino acid mutagenesis studies, targeting residues both within and outside the 77–83 Bw4 and Bw6 sequence motifs, have previously identified critical amino acids that contribute to alloantibody binding [31,34,35]. Specifically, following extensive *in vitro* single residue mutations (substituting Bw6 specific residues with those found at the same sequence position in the Bw4 motif) amino acids 79, 82, and 83 were shown to be critical components of the Bw6 epitope [31]. Mutations R79G and R82L introduced in HLA-B\*07:02 sequence abrogated Bw6 monoclonal antibody binding, whereas mu-

tation R82L also led to loss of Bw6 specific alloantibody reactivity. Similarly, mutation G83R abrogated both Bw6 specific monoclonal antibody and alloantibody binding to HLA-B\*07:02. Substitution N80T, however, did not affect Bw6 specific monoclonal antibody reactivity, indicating that amino acid polymorphism at position 80 may not significantly alter the Bw6 epitope structure [31].

The effect of the above single amino acid substitutions on the 3D surface electrostatic pattern of HLA-B\*07:02 mutants are shown in Fig. 5. Residues Arg79, Arg82, and Gly83 are oriented outward and constitute most of the molecular surface of the Bw6 epitope (Table

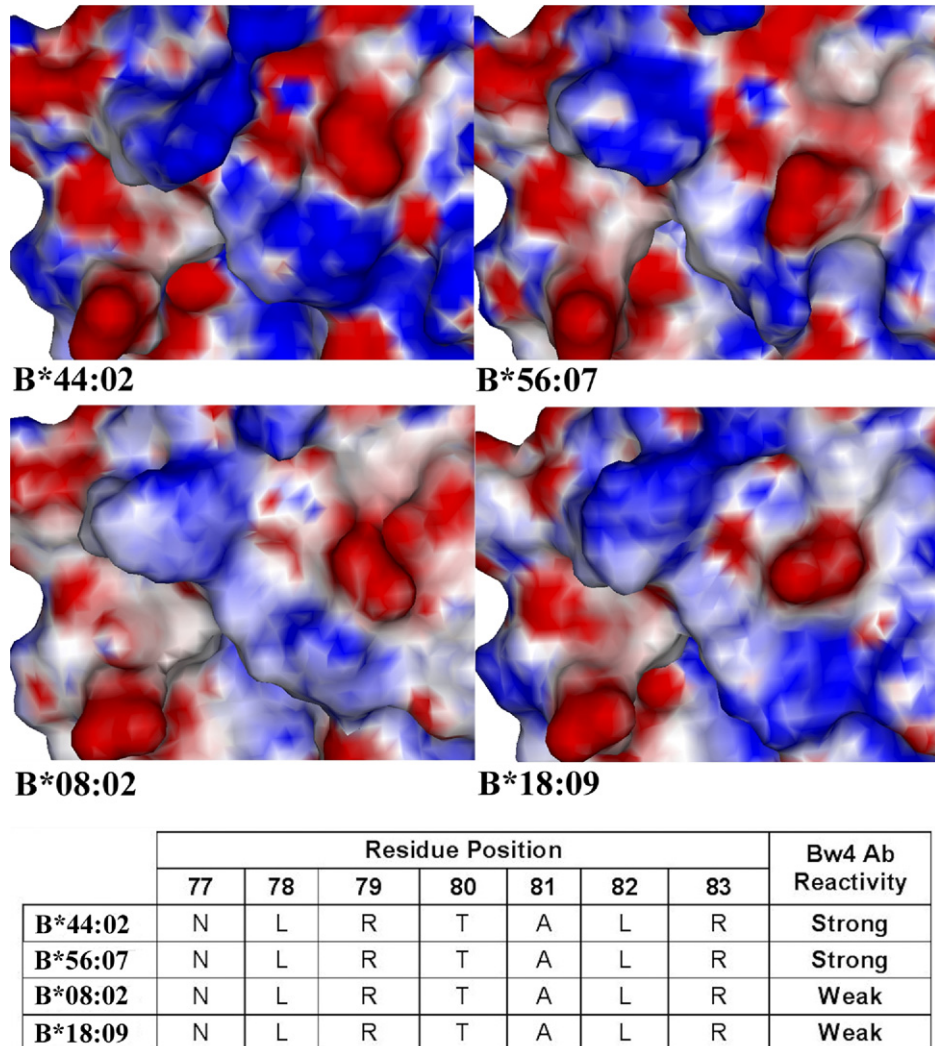


**Fig. 4.** Variation in the electrostatic properties of Bw4 epitope despite identity at the amino acid sequence level. The same view of Bw4 epitope as in Fig. 3 is shown. HLA-B\*44:02, B\*56:07, B\*08:02 and B\*18:09 possess an identical Bw4 sequence motif but showed different reactivity with Bw4 specific antibody.

2). Mutations R79G and R82L result in a net reduction in the exposed epitope surface area (from 367 Å<sup>2</sup> for HLA-B\*07:02 to 257 Å<sup>2</sup> for the R79G variant and 313 Å<sup>2</sup> for the R82L variant), and significantly alter the epitope conformation. In contrast, G83R substitution increases the solvent-accessible area of the epitope (to a total of 419 Å<sup>2</sup>) and may therefore abrogate antibody binding by steric hindrance. Importantly, mutations at positions 79, 82, and 83 markedly alter the electrostatic properties of the Bw6 epitope, providing a structural explanation for the results of mutagenesis studies. Conversely, substitution of asparagine to threonine at position 80 has minimal effect on the electrostatic pattern and total solvent-accessible surface (from 367 to 354 Å<sup>2</sup>) of Bw6, and would not, therefore, be expected to disrupt the antibody paratope-Bw6 epitope association.

#### 4. Discussion

The potential of HLA alloantigens to stimulate humoral immune responses in the context of transplantation depends on the presence and nature of amino acid polymorphisms between donor and recipient HLA molecules. Previous studies by ourselves and others have shown that simply enumerating the number of polymorphic amino acids at continuous and discontinuous sequence positions is useful for predicting the relative immunogenicity of individual HLA mismatches after exposure to alloantigen [3–5,36]. The use of se-

quence information alone, however, provides limited insight into key determinants of B cell epitope immunogenicity, such as the orientation, accessibility, and physiochemical properties of amino acid side chains.

In the present study, we used comparative protein structure modeling to generate high-resolution 3D structural and physicochemical models of all common HLA class I alleles. The resulting high-resolution models provide a new basis for defining HLA immunogenicity and allow novel insights into HLA class I B cell epitopes. Because electrostatic charge is the major determinant of protein–protein interactions and electrostatic forces are key mediators of high-affinity antibody–antigen binding, we performed a comprehensive analysis of the electrostatic potential at the surface of individual HLA molecules accounting for the number and distribution of polar and charged amino acid side chains and the fold and structural composition of each protein. The modeling methodology used in the present study is well established [13,37] and a rigorous approach was used for the selection of appropriate global templates from which to model the most commonly occurring HLA-A, -B, and -C molecules. The protein structures generated from the selected templates performed well when subjected to stereochemical and energy based testing of their structural integrity.

Application of the models to examine serologically defined HLA class I epitopes confirmed that the molecular models of HLA class I

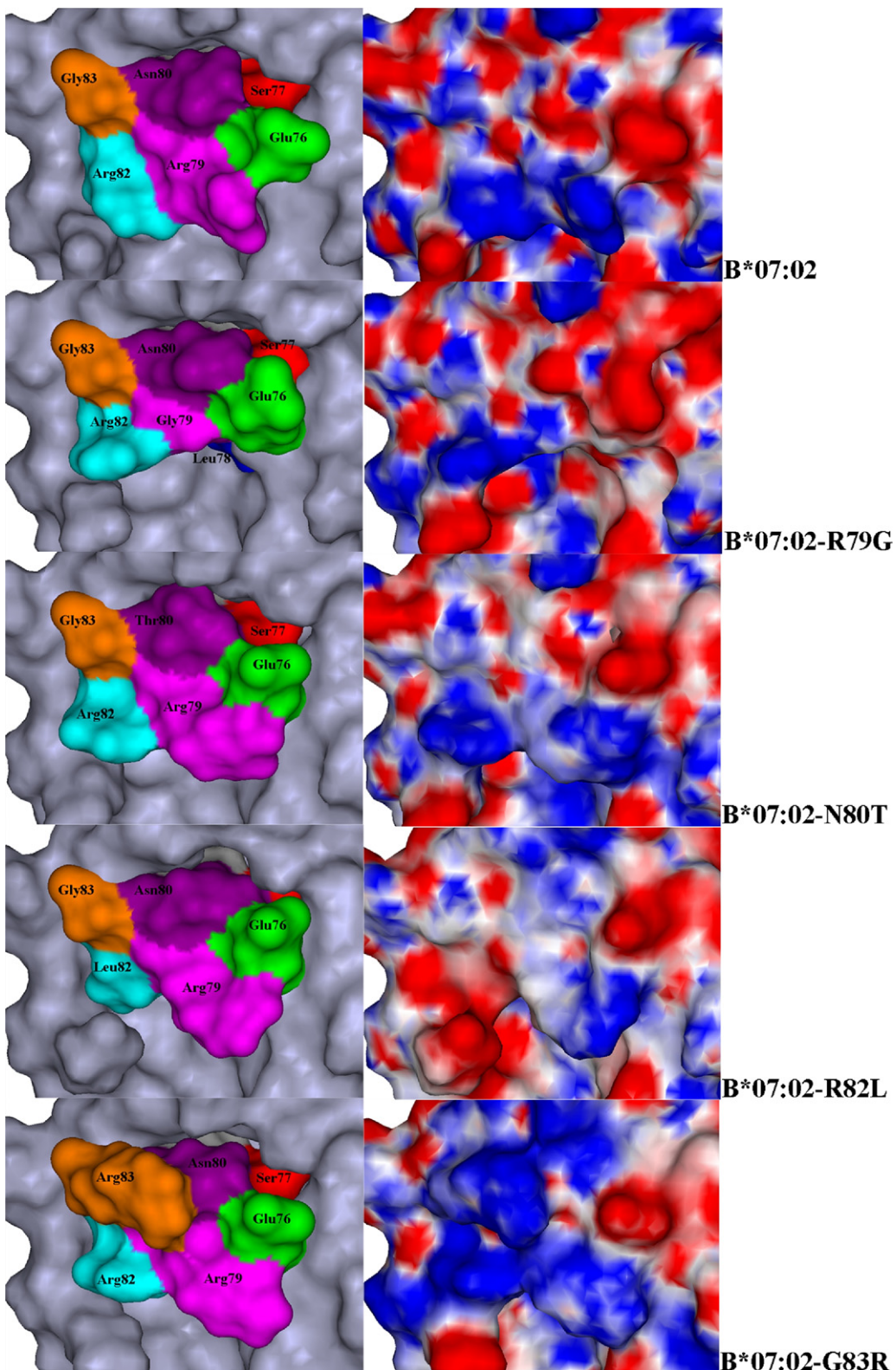


**Fig. 5.** Effect of point residue mutations on Bw6 epitope electrostatic properties. The images show the “birds-eye-view” of Bw6 epitope (as for Fig. 1). All structures were superimposed on HLA-B\*07:02. The mutations described were introduced into the sequence of HLA-B\*07:02 and the tertiary structures were computed using homology modeling; the electrostatic potential was then calculated (methods). The left side column depicts the solvent accessible surface of the epitope which was colored to reveal the contributions of the relevant residues, whereas the surface of the rest of molecule was colored in gray. The molecular surface was also colored according to the calculated electrostatic potential (as explained previously; right side column). Mutations at positions R79G, R82L, and G83R markedly alter the electrostatic properties of the Bw6 epitope; conversely, mutation N80T has minimal effect on the electrostatic motif of the epitope.

**Table 2**

Solvent accessibility of Bw6 epitope residues for HLA-B\*07:02 and single amino acid variants

	76 E	77 S	78 L	79 R	80 n	81 L	82 R	83 G
<b>B*07: 02</b>								
SAS ( $\text{\AA}^2$ )	85.6	7.1	5.5	125.1	43.9	2.5	70.9	26.2
%SAS	41.9	5.1	5.3	53.3	28.5	1.3	27.4	47.9
<b>B*07: 02-R79G</b>								
SAS ( $\text{\AA}^2$ )	91.7	10	2.5	18.1	38.7	0.5	70.4	24.7
%SAS	51.2	7.2	4.2	30.8	24.5	0.3	29.6	46.3
<b>B*07: 02-N80T</b>								
SAS ( $\text{\AA}^2$ )	85.8	6.3	6.5	125.5	25.5	1.0	79	24.7
%SAS	43.3	5.1	7.4	53.2	23	0.5	31.9	45.1
<b>B*07: 02-R82L</b>								
SAS ( $\text{\AA}^2$ )	79	7.3	1.5	150.6	22.4	13.1	12.6	26.2
%SAS	40.1	5.3	1.3	65	18.2	6.9	6.7	46.5
<b>B*07: 02-G83R</b>								
SAS ( $\text{\AA}^2$ )	86.7	6.8	6.5	112.4	9.6	3	67.1	126.6
%SAS	43	5.2	3.9	44	5.4	1.6	27.4	59.2

Table shows the SAS of the named residues. %SAS denotes the residue solvent accessibility in the structure divided by the residue solvent accessibility of the fully exposed residue (methods).

were functionally accurate representations of the tertiary proteins. The two B cell epitopes selected for study (Bw4 and Bw6) are both widely expressed and were chosen for analysis because they have been particularly well characterized using conventional serologic techniques and amino acid mutagenesis studies to define antibody binding patterns. In both cases the structural models created provided an explanation, in terms of physicochemical determinants, for the different patterns of antibody binding previously identified.

The concept of an electrostatic motif, defined as a distinct topographic pattern of electrostatic potential in 3D space, shared among macromolecules of similar structure has provided a powerful tool for the identification of functionally important regions on the surface of proteins [11,12]. Such common structural and electrostatic motifs may be conserved between proteins despite the absence of a corresponding shared sequence motif. The analyses of electrostatic properties of Bw4 and Bw6 epitopes presented in this study suggest a similar finding. The electrostatic pattern and conformation of each epitope are maintained among HLA molecules even though they are expressed in a different structural context. Importantly, variation in the amino acid composition of the epitope does not always translate into a different electrostatic motif (e.g., Bw4 epitope), providing a possible mechanism for observed patterns of serologic cross-reactivity. Mutations, however, of critical amino acids that lead to abrogation of antibody binding also induce dramatic changes on the electrostatic properties of the epitope.

It is important to acknowledge a number of potential limitations of the current study. HLA class I molecules bind a broad range of linear peptides in their peptide binding groove and, together with  $\beta$ 2-microglobulin, these help maintain the integrity of the tertiary structure. For the purpose of comparative modeling, we incorporated an alanine nonamer in the peptide binding groove to enable appropriate orientation of the amino acid side chains lining the groove and for accurate prediction of the groove architecture, as well as to simulate the effects of solvent inaccessible residues on the surface electrostatic potential and accurately depict the molecular surface. Alanine was chosen because it does not alter the main chain conformation and does not impose electrostatic or steric

effects limiting, therefore, any effect of the bound peptide on the rest of the HLA molecule [38]. Although the nature of the peptide bound to HLA class I may be a critical determinant for recognition by alloreactive T cells, the significance of the amino acid sequence of the bound peptide on alloantibody binding is inconclusive. Alloantibodies bind to B cell epitopes determined by polymorphic residues carried almost exclusively by the HLA class I heavy chain [39]. However, Mulder et al. showed that the reactivity of certain human monoclonal antibodies may be peptide dependent, and Takamiya et al. suggested that the presence of a charged peptide residue at pocket P8 had a significant effect on the reactivity of a Bw4 specific monoclonal antibody [40,41]. It is also important to recognize that part of the heterogeneity in the observed antibody reactivity against certain epitopes, such as Bw4, may also be attributed to the requirement of a secondary antibody binding site which, in conjunction with the primary epitope, stabilizes the antibody–antigen interaction [42]. Indeed, Duquesnoy et al. suggested that the reactivity pattern of a Bw4 specific antibody (which showed positive reactions against most Bw4 HLA molecules, including HLA-A23, -A24, and -A32, but negative reactions against HLA-A25 and -B13) could be explained by the combination of a primary (Bw4) and a secondary binding site, the latter being absent on the nonreactive Bw4-expressing HLA molecules [43].

Another limitation of the protein modeling approach used in the present study is that the effects of protein glycosylation were not considered. Glycosylation is not a major determinant of immunogenicity although there are reported examples of glycosylated residues influencing binding of HLA specific alloantibodies [44]. Finally, although protein electrostatic properties are the principal determinant of antibody binding, additional factors such as hydrophobic interactions, surface accessible area, and steric conformation are also critical for effective antibody–antigen engagement [45,46].

Our intention in future studies is to quantify the 3D electrostatic potential on the surface of HLA and to examine whether quantitative differences among HLA molecules better reflect their immunogenic potential in the context of organ transplantation. The HLA class I modeling approach described may also aid the prediction of other aspects of HLA function, including, for example, the study of leukocyte receptor ligands and analysis of the extent to which different peptides within the peptide binding groove influence the topography of the HLA molecule [40].

In conclusion, the use of high-resolution structural modeling has emphasized the link between the electrostatic potential on the surface of HLA B cell epitopes in relation to antibody–antigen interactions; this structural and physicochemical approach may lead to a better definition of donor/recipient compatibility in the context of organ transplantation.

#### Acknowledgments

This study was supported by the NIHR Cambridge Biomedical Research Centre. The authors thank Dr Peter J. Winn, Centre for Systems Biology, University of Birmingham (Birmingham, UK), for critical reading of this manuscript.

#### Appendix. Supplementary data

Supplementary data associated with this article can be found, in the online version, at [10.1016/j.humimm.2011.07.303](https://doi.org/10.1016/j.humimm.2011.07.303).

#### References

- [1] Bjorkman PJ, Saper MA, Samraoui B, Bennett WS, Strominger JL, Wiley DC. Structure of the human class I histocompatibility antigen, HLA-A2. *Nature* 1987;329:506–12.
- [2] Brown JH, Jardetzky TS, Gorga JC, et al. Three-dimensional structure of the human class II histocompatibility antigen HLA-DR1. *Nature* 1993;364:33–9.
- [3] Duquesnoy RJ. HLAMatchmaker: A molecularly based algorithm for histocompatibility determination. I. Description of the algorithm. *Hum Immunol* 2002; 63:339–52.

- [4] Kosmoliaptis V, Bradley JA, Sharples LD, et al. Predicting the immunogenicity of human leukocyte antigen class I alloantigens using structural epitope analysis determined by HLA Matchmaker. *Transplantation* 2008;85:1817–25.
- [5] Kosmoliaptis V, Chaudhry AN, Sharples LD, et al. Predicting HLA class I alloantigen immunogenicity from the number and physicochemical properties of amino acid polymorphisms. *Transplantation* 2009;88:791–8.
- [6] Sinha N, Smith-Gill SJ. Electrostatics in protein binding and function. *Curr Protein Pept Sci* 2002;3:601–14.
- [7] Nakamura H. Roles of electrostatic interaction in proteins. *Q Rev Biophys* 1996;29:1–90.
- [8] Sharp KA, Honig B. Electrostatic interactions in macromolecules: Theory and applications. *Annu Rev Biophys Biophys Chem* 1990;19:301–32.
- [9] Slagle SP, Kozack RE, Subramanian S. Role of electrostatics in antibody-antigen association: Anti-hen egg lysozyme/lysozyme complex (HyHEL-5/HEL). *J Biomol Struct Dyn* 1994;12:439–56.
- [10] Chong LT, Duan Y, Wang L, Massova I, Kollman PA. Molecular dynamics and free-energy calculations applied to affinity maturation in antibody 4G8G7. *Proc Natl Acad Sci U S A* 1999;96:14330–5.
- [11] Honig B, Nicholls A. Classical electrostatics in biology and chemistry. *Science* 1995;268:1144–9.
- [12] Botti SA, Felder CE, Sussman JL, Electrotactins SI. A class of adhesion proteins with conserved electrostatic and structural motifs. *Protein Eng* 1998;11:415–20.
- [13] Sali A, Blundell TL. Comparative protein modelling by satisfaction of spatial restraints. *J Mol Biol* 1993;234:779–815.
- [14] Altschul SF, Madden TL, Schäffer AA, et al. Gapped BLAST and PSI-BLAST: A new generation of protein database search programs. *Nucleic Acids Res* 1997;25:3389–402.
- [15] Hooft RW, Vriend G, Sander C, Abola EE. Errors in protein structures. *Nature* 1996;381:272.
- [16] Laskowski RA, MacArthur MW, Moss D, PROCHECK TJM. A program to check the stereochemical quality of protein structures. *J Appl Crystallogr* 1993;26:283–91.
- [17] Ramachandran GN. Protein Structure and crystallography. *Science* 1963;141:288–91.
- [18] Ramachandran GN, Ramakrishnan C, Sasisekharan V. Stereochemistry of polypeptide chain configurations. *J Mol Biol* 1963;7:95–9.
- [19] Thompson JD, Gibson TJ, Plewniak F, Jeanmougin F, Higgins DG. The CLUSTAL\_X Windows interface: Flexible strategies for multiple sequence alignment aided by quality analysis tools. *Nucleic Acids Res* 1997;25:4876–82.
- [20] MacKerell ADJ, Bashford D, Bellott M, et al. All-atom empirical potential for molecular modeling and dynamics studies of proteins. *J Phys Chem B* 1998;102:3586–616.
- [21] Clore GM, Brünger AT, Karplus M, Gronenborn AM. Application of molecular dynamics with interproton distance restraints to three-dimensional protein structure determination. A model study of crambin. *J Mol Biol* 1986;191:523–51.
- [22] Rocchia W, Alexov E, Honig B. Extending the applicability of the nonlinear Poisson-Boltzmann equation: Multiple dielectric constants and multivalent ions. *J Phys Chem B* 2001;105:6507–14.
- [23] Rocchia W, Sridharan S, Nicholls A, Alexov E, Chiabrera A, Honig B. Rapid grid-based construction of the molecular surface and the use of induced surface charge to calculate reaction field energies: Applications to the molecular systems and geometric objects. *J Comput Chem* 2002;23:128–37.
- [24] Sippl MJ. Recognition of errors in three-dimensional structures of proteins. *Proteins* 1993;17:355–62.
- [25] Sippl MJ. Knowledge-based potentials for proteins. *Curr Opin Struct Biol* 1995;5:229–35.
- [26] Wan AM, Ennis P, Parham P, Holmes N. The primary structure of HLA-A32 suggests a region involved in formation of the Bw4/Bw6 epitopes. *J Immunol* 1986;137:3671–4.
- [27] Müller CA, Engler-Blum G, Gekeler V, Steiert I, Weiss E, Schmidt H. Genetic and serological heterogeneity of the supertypic HLA-B locus specificities Bw4 and Bw6. *Immunogenetics* 1989;30:200–7.
- [28] Vilches C, de Pablo R, Herrero MJ, Moreno ME, Kreisler M. HLA-B73: An atypical HLA-B molecule carrying a Bw6-epitope motif variant and a B pocket identical to HLA-B27. *Immunogenetics* 1994;40:166.
- [29] Balas A, García-Sánchez F, Santos S, Lillo R, Merino JL, Vicario JL. Characterization of a new HLA-B18 allele, B\*1806, which lacks expression of the Bw6 epitope. *Tissue Antigens* 1998;52:579–82.
- [30] Voorter CE, van der Vlies S, Kik M, van den Berg-Loonen EM. Unexpected Bw4 and Bw6 reactivity patterns in new alleles. *Tissue Antigens* 2000;56:363–70.
- [31] Lutz CT, Smith KD, Greazel NS, et al. Bw4-reactive and Bw6-reactive antibodies recognize multiple distinct HLA structures that partially overlap in the alpha-1 helix. *J Immunol* 1994;153:4099–110.
- [32] Collins RW, Harmer AW, Heads AJ, Kondeatis E, Page G, Vaughan RW. The clinical importance of variation within the HLA-Bw4 complex. *Transplantation* 2001;72:1851–3.
- [33] Arnett KL, Adams EJ, Gumperz JE, et al. Expression of an unusual Bw4 epitope by a subtype of HLA-B8 [B\*0802]. *Tissue Antigens* 1995;46:316–21.
- [34] Toubert A, Raffoux C, Boretto J, et al. Epitope mapping of HLA-B27 and HLA-B7 antigens by using intradomain recombinants. *J Immunol* 1988;141:2503–9.
- [35] Parham P, Antonelli P, Herzenberg LA, Kipps TJ, Fuller A, Ward FE. Further studies on the epitopes of HLA-B7 defined by murine monoclonal antibodies. *Hum Immunol* 1986;15:44–67.
- [36] Duquesnoy RJ. A structurally based approach to determine HLA compatibility at the humoral immune level. *Hum Immunol* 2006;67:847–62.
- [37] Sánchez R, Pieper U, Melo F, et al. Protein structure modeling for structural genomics. *Nat Struct Biol* 2000;7:suppl:986–90.
- [38] Cunningham BC, Wells JA. High-resolution epitope mapping of hGH-receptor interactions by alanine-scanning mutagenesis. *Science* 1989;244:1081–5.
- [39] Barnardo MC, Harmer AW, Shaw OJ, et al. Detection of HLA-specific IgG antibodies using single recombinant HLA alleles: The MonoLISA assay. *Transplantation* 2000;70:531–6.
- [40] Mulder A, Eijsink C, Kester MG, et al. Impact of peptides on the recognition of HLA class I molecules by human HLA antibodies. *J Immunol* 2005;175:5950–7.
- [41] Takamiya Y, Sakaguchi T, Miwa K, Takiguchi M. Role of HLA-B\*5101 binding nonamer peptides in formation of the HLA-Bw4 public epitope. *Int Immunol* 1996;8:1027–34.
- [42] Duquesnoy RJ, Mulder A, Askar M, Fernandez-Vina M, Claas FH. HLA Matchmaker-based analysis of human monoclonal antibody reactivity demonstrates the importance of an additional contact site for specific recognition of triplet-defined epitopes. *Hum Immunol* 2005;66:749–61.
- [43] Marrari M, Mostecki J, Mulder A, Claas F, Balazs I, Duquesnoy RJ. Human monoclonal antibody reactivity with human leukocyte antigen class I epitopes defined by pairs of mismatched eplets and self-eplets. *Transplantation* 2010;90:1468–72.
- [44] Sparrow RL, Vaughan HA, McKenzie IF. Human class II antigens. Implication of carbohydrate in the determinants recognized by several antihuman class II monoclonal antibodies. *Transplantation* 1986;42:647–52.
- [45] Jones S, Thornton JM. Principles of protein–protein interactions. *Proc Natl Acad Sci U S A* 1996;93:13–20.
- [46] Sundberg EJ, Urrutia M, Braden BC, et al. Estimation of the hydrophobic effect in an antigen–antibody protein–protein interface. *Biochemistry* 2000;39:15375–87.